PERGAMON

International Journal of Engineering Science 39 (2001) 737–754

International Journal of Engineering Science

www.elsevier.com/locate/ijengsci

Stress relaxation during creep of rocks around deep boreholes

Iuliana Paraschiv-Munteanu [a,*], N.D. Cristescu [b]

[a] *Faculty of Mathematics, Department of Mechanics, University of Bucharest, Str. Academiei, 14, Bucharest 70109, Romania*

[b] *Department of Aerospace Engineering, Mechanics and Engineering Science, 231 Aerospace Building, P.O. Box 116250, Gainesville, FL 32611-6250, USA*

Received 31 March 2000; accepted 31 March 2000

(Communicated by E. SOÓS)

Abstract

The variation of stress during creep convergence of a deep borehole excavated in rock salt is examined. A non-associated elasto/viscoplastic constitutive equation is used to describe both compressibility and/or dilatancy during transient and steady-state creep, as well as evolutive damage possibly leading to failure. An in-house FEM numerical method is used for this purpose. The variation in time of radial convergence of the borehole walls and of the stress state (at various distances from the borehole surface) is illustrated by several figures. The significance of these variations for long-term stability is discussed.

1. Introduction

The stress distribution around a deep borehole has been studied by very many authors. The problem has a great importance for petroleum industry, mainly for welbore stability [21] as well as for mining industry [19,20]. Various initial assumptions have been chosen, as well as several mechanical models to describe the behavior of the rocks. Quite often linear elasticity was used together with the assumption of plane stress state (see [6,10,16], among others). However, for very deep boreholes, if the two ends are disregarded, the problem can be approached as a plane strain problem, involving all stress components. Also, in order to describe creep and wall convergence rheological models are necessary. Thus, Massier and Cristescu [14] have used simplified viscoelastic and viscoplastic models to describe creep around a borehole. More general viscoelastic

* Corresponding author. Tel.: + 40-1-6844192.
E-mail address: pmiulia@math.math.unibuc.ro (I. Paraschiv-Munteanu).

0020-7225/01/$ - see front matter
PII: S0020-7225(00)00060-4

model describing volumetric creep as well, has been used by Massier [12,13]. These models can describe compressibility only. For rocks which are compressible for some stress states, but dilatant for some other stress states, elasto/viscoplastic models were used ([1,2]; see also [3,11]).

The stress state just after the drilling is obtained as an elastic instantaneous solution. With a viscoplastic non-associated model this allows us to find out afterwards where around the borehole the rock becomes dilatant, where compressible and where a possible failure can be expected. In the same manner the beginning of the rock creep can be studied, the location where a fast creep will take place as well as where evolutive damage is to be expected (see e.g. [5, Chapter 8] and [17]). A variety of cases were considered in the above-mentioned papers, what concerns the type of rocks, depth, far field stress distribution, inner pressure, etc. The formulae, used to describe creep of a compressible/dilatant viscoplastic rock, with the assumption that the stresses remain constant during creep, are very simple and thus, easy to apply. They may describe well the beginning of the creep process but for a longer period of time and for great depth one has to take into account that during long periods of time following the drilling, the stresses may vary, due to non-uniform stress distribution, the presence of far field stresses and of a borehole which changes geometry.

In the present paper, we are dealing with the stress variation during creep of rock salt around a deep borehole. Various far field stress distributions are considered, several depths and various pressures exerted on the inner surface. Since the system of equations governing this problem is quite involved, numerical methods (FEM) are used, as developed by Ionescu and Sofonea [8] and Paraschiv-Munteanu [18]. Another numerical approach to the same problem, also for rock salt, is due to Glabisch [7] using someother FEM code. A study of stress relaxation in rock salt surrounding a deep borehole using FEM, has been done also by Jin and Cristescu [9]; another non-associated elastic/viscoplastic constitutive equation for rock salt than in the present paper was used, in which only the transient term was taken into account. The stress variation obtained shows a decrease in time of octahedral shear stress with respect to the elastic solution, in the neighborhood of the orifice, but an increase at farer distances.

Finite differences were also used to study the stress variation during creep of other rocks: for andesite [1], granite [2], coal [3], where, however associated elastic/viscoplastic constitutive equations have been used and only some aspects of stress relaxation have been studied. However, as a general conclusion, for very long time intervals one has to take into account the stress variation during creep, in order to correctly predict stability, wall convergence, damage, and possible failure taking place after long time intervals following the drilling.

2. The constitutive equation

The constitutive equation is of a non-associated elastic-viscoplastic type [3]. The reference configuration, with respect to which the strains must be estimated, is the state in situ before excavation, there where the future excavation is envisaged. Using standard notation we have for the rate of deformation tensor

$$\dot{\boldsymbol{\varepsilon}} = \frac{\dot{\boldsymbol{\sigma}}^{\mathrm{R}}}{2G} + \left(\frac{1}{3K} - \frac{1}{2G}\right)\dot{\sigma}^{\mathrm{R}}\mathbf{1} + k_{\mathrm{T}}\left\langle 1 - \frac{W^{\mathrm{I}}(t)}{H(\boldsymbol{\sigma})}\right\rangle \frac{\partial F}{\partial \boldsymbol{\sigma}}(\boldsymbol{\sigma}) + k_{\mathrm{S}}\frac{\partial S}{\partial \boldsymbol{\sigma}}(\boldsymbol{\sigma}), \tag{1}$$

where G and K are elastic moduli which may depend on the invariants of stress and strain and possibly on the damage of rock, [1] $H(\boldsymbol{\sigma}(t)) = W^{\mathrm{I}}(t)$ is the equation of the stabilization boundary for the transient creep, $F(\boldsymbol{\sigma})$ and $S(\boldsymbol{\sigma})$ are the viscoplastic potentials for the transient and steady-state creep, respectively, k_{T} and k_{S} are the corresponding viscosity coefficients, $\mathbf{1}$ the unit tensor and $\sigma = (1/3)(\sigma_1 + \sigma_2 + \sigma_3)$ is the mean stress. We will use the notation τ for the octahedral shear stress:

$$\tau = \frac{\sqrt{2}}{3}\overline{\sigma} \quad \text{with } \overline{\sigma}^2 = \sigma_1^2 + \sigma_2^2 + \sigma_3^2 - \sigma_1\sigma_2 - \sigma_2\sigma_3 - \sigma_3\sigma_1,$$

the "equivalent" stress. In (1), the work-hardening parameter (the internal state variable) is the irreversible stress work per unit volume:

$$W^{\mathrm{I}}(t) = W^{\mathrm{P}} + \int_0^t \sigma(s)\dot{\varepsilon}_{\mathrm{v}}^{\mathrm{I}}(s)\,\mathrm{d}s + \int_0^t \boldsymbol{\sigma}'(s) \cdot \left(\dot{\boldsymbol{\varepsilon}}^{\mathrm{I}}\right)'(s)\,\mathrm{d}s, \tag{2}$$

where $t = 0$ is the moment of excavation and the W^{P} is the primary (initial) value of W^{S} [3]. In (2), $\varepsilon_{\mathrm{v}}^{\mathrm{I}}$ is the irreversible part of the volumetric deformation and $(\dot{\boldsymbol{\varepsilon}}^{\mathrm{I}})'$ is the deviator of the irreversible part of the rate of deformation tensor. Finally, the bracket $\langle\ \rangle$ from (1) has the meaning of the positive part of the function mentioned, i.e.,

$$\langle A \rangle = A^{+} = \frac{1}{2}(A + |A|).$$

All constitutive functions and parameters involved in (1) are determined from experimental data. The constitutive equation (1) can describe the following mechanical properties exhibited by most rocks: transitory and steady-state creep, work-hardening during transient creep, volumetric compressibility and/or dilatancy, as well as short-term failure. All these properties are incorporated into the constitutive equation via the procedure used to determine the constitutive functions [3–5]. Example of expressions for the constitutive functions obtained for rock salt and used in this paper for numerical calculus is given in Appendix A.

3. Mathematical formulation of the problem

We show shortly how can be found the stress distribution around a circular vertical cavity excavated in rock salt. We formulate the problem as it will be used in the numerical integration described below. If the cavity has the initial radius a and if on its walls

$$\Gamma_1 = \{(a, \theta) \mid \theta \in [0, 2\pi)\}, \tag{3}$$

[1] Recent experimental results have shown that the elastic parameters of rock salt are depending mainly on the irreversible volumetric strain, or on the history of variation of the irreversible volumetric strain [15].

a pressure p is acting (due to various reasons and which may be constant or variable), the stress state just after excavations is

$$\begin{aligned}
\tilde{\sigma}^{\mathrm{S}}_{rr}(r) &= \left[\tilde{N} + (1-\tilde{N})\frac{a^2}{r^2}\right](p-\sigma_{\mathrm{h}}) + \sigma_{\mathrm{h}},\\
\tilde{\sigma}^{\mathrm{S}}_{\theta\theta}(r) &= \left[\tilde{N} - (1-\tilde{N})\frac{a^2}{r^2}\right](p-\sigma_{\mathrm{h}}) + \sigma_{\mathrm{h}},\\
\tilde{\sigma}^{\mathrm{S}}_{zz}(r) &= \frac{3K-2G}{G+3K}\tilde{N}(p-\sigma_{\mathrm{h}}) + \sigma_{\mathrm{v}},\\
\tilde{\sigma}^{\mathrm{R}}_{r\theta} &= \tilde{\sigma}^{\mathrm{R}}_{rz} = \tilde{\sigma}^{\mathrm{R}}_{\theta z} = 0,
\end{aligned} \tag{4}$$

where

$$\tilde{N} = \frac{1}{1+(3G/(G+3K))m^2}$$

with $m \in \mathbf{N}$, $m \geqslant m_0 \geqslant 5$, number of radiuses which defined the limits of the domain, where solution is found:

$$\Omega = [a, ma] \times [0, 2\pi), \tag{5}$$

σ_{h} and σ_{v} are the horizontal and vertical initial (primary) stresses (the "far field stresses"), $\sigma_{\mathrm{h}} = n\sigma_{\mathrm{v}}$ with $n =$ constant, and generally $0.3 \leqslant n < 3$ is the interval most often found underground. A solution of the problem in the finite domain (5) will be denoted by a "tilde". We assume that in all horizontal directions the primary stresses are the same.

The corresponding deformation are

$$\begin{aligned}
\tilde{\varepsilon}_{rr}(r) &= \frac{1}{2G}\left[\tilde{C}\tilde{N} + (1-\tilde{N})\frac{a^2}{r^2}\right](p-\sigma_{\mathrm{h}}),\\
\tilde{\varepsilon}_{\theta\theta}(r) &= \frac{1}{2G}\left[\tilde{C}\tilde{N} - (1-\tilde{N})\frac{a^2}{r^2}\right](p-\sigma_{\mathrm{h}}),
\end{aligned} \tag{6}$$

where

$$\tilde{C} = \frac{3G}{G+3K},$$

with all the other components zero. From here it is easy to obtain the radial component of the displacement (the other components are zero):

$$\tilde{u} = \frac{1}{2G}\left[\left(1 - \frac{3K-2G}{G+3K}\right)\tilde{N} - (1-\tilde{N})\frac{a^2}{r^2}\right] r(p-\sigma_{\mathrm{h}}). \tag{7}$$

It is obvious that deformation and displacement components are zero on the external boundary of the domain Ω:

$$\Gamma_2 = \{(ma, \theta) \mid \theta \in [0, 2\pi)\}. \tag{8}$$

Remarks

1. *It is easy to observe that in the case of infinite domain, when $m \to \infty$, the stresses, deformation and displacement components are the same like in the papers of Cristescu* [3]*, Paraschiv and Cristescu* [17].
2. *For the bounded domain (like the one considered in this paper) the mean stress is:*

$$\tilde{\sigma}^{\mathrm{R}} = \frac{3K}{G + 3K}\tilde{N}(p - \sigma_{\mathrm{h}}) \neq 0.$$

   In case of the unbounded domain (when $m \to \infty$) we get $\tilde{\sigma}^{\mathrm{R}} = 0$, i.e., in each plain $z =$ constant, the stress state at each point remains in the same octahedral plain.
3. *Concerning the constant $\tilde{N}$ we obtain $\tilde{N} \to 0$ when $m \to \infty$. This result shows that taking $m \geqslant m_0 \geqslant 5$ is acceptable approach for the formulation at the finite boundary $r = ma$ of the boundary conditions from infinity.*

The general formulation of the problem of determining the stress distribution around a circular vertical cavity in elasto-viscoplastic rock, considered a cvasistatic problem, is:

Find the displacement function $u: \mathbf{R}_+ \times [a, ma] \to \mathbf{R}$, the stress function $\boldsymbol{\sigma}: \mathbf{R}_+ \times [a, ma] \to \mathscr{S}_3$ and the irreversible stress work function $W^{\mathrm{I}}: \mathbf{R}_+ \times [a, ma] \to \mathbf{R}$ such that:

$$\operatorname{Div} \boldsymbol{\sigma}^{\mathrm{R}}(t, r) = 0 \quad \text{in } \mathbf{R}_+ \times [a, ma], \tag{9}$$

$$\begin{aligned}\dot{\boldsymbol{\sigma}}^{\mathrm{R}} = {} & 2G\dot{\boldsymbol{\varepsilon}} + (3K - 2G)\dot{\varepsilon}\mathbf{1} + k_{\mathrm{T}}\left\langle 1 - \frac{W^{\mathrm{I}}(t)}{H(\boldsymbol{\sigma})}\right\rangle\left[\frac{(2G - 3K)}{3}\frac{\partial F}{\partial \sigma}\mathbf{1} - 2G\frac{\partial F}{\partial \boldsymbol{\sigma}}\right] \\ & + k_{\mathrm{S}}\left[\frac{(2G - 3K)}{3}\frac{\partial S}{\partial \sigma}\mathbf{1} - 2G\frac{\partial S}{\partial \boldsymbol{\sigma}}\right] \quad \text{in } \mathbf{R}_+ \times [a, ma],\end{aligned} \tag{10}$$

$$\dot{W}^{\mathrm{I}} = k_{\mathrm{T}}\left\langle 1 - \frac{W^{\mathrm{I}}(t)}{H(\boldsymbol{\sigma})}\right\rangle \frac{\partial F}{\partial \boldsymbol{\sigma}} \cdot \boldsymbol{\sigma} + k_{\mathrm{S}}\frac{\partial S}{\partial \boldsymbol{\sigma}} \cdot \boldsymbol{\sigma} \quad \text{in } \mathbf{R}_+ \times [a, ma], \tag{11}$$

$$\begin{cases} \sigma^{\mathrm{R}}_{rr}(t, a) = p - \sigma^{\mathrm{P}}_{rr}, \quad \sigma^{\mathrm{R}}_{r\theta}(t, a) = \sigma^{\mathrm{R}}_{rz}(t, a) = 0, \quad (\forall)t > 0 \ \ (\text{on } \Gamma_1), \\ u(t, ma) = 0, \quad (\forall)t > 0 \ \ (\text{on } \Gamma_2), \end{cases} \tag{12}$$

$$\begin{cases} \boldsymbol{\sigma}^{\mathrm{S}}(0, r) = \boldsymbol{\sigma}^{\mathrm{P}} + \tilde{\boldsymbol{\sigma}} \quad \text{or} \quad \boldsymbol{\sigma}^{\mathrm{R}}(0, r) = \tilde{\boldsymbol{\sigma}}, \\ u(0, r) = \tilde{u}, \qquad\qquad (\forall)r \in [a, ma], \\ W^{\mathrm{I}}(0, r) = H(\boldsymbol{\sigma}^{\mathrm{P}}), \end{cases} \tag{13}$$

where $\tilde{\boldsymbol{\sigma}}$ and $\tilde{u}$ are the stress and the displacement, respectively, corresponding to the moment of excavation and $\sigma_{rr}^{\mathrm{P}} = \sigma_{\mathrm{h}}$. The superscript $^{\mathrm{R}}$ stays for "relative" and $^{\mathrm{S}}$ for "secondary"; the stress after excavation is $\boldsymbol{\sigma}^{\mathrm{S}}$ while $\boldsymbol{\sigma}^{\mathrm{R}} = \boldsymbol{\sigma}^{\mathrm{S}} - \boldsymbol{\sigma}^{\mathrm{P}}$ and it is just this last relative component which produces the deformation with respect to the state before excavation.

4. The numerical approach

For the problem (9)–(13), we determine a numerical solution based on some results presented by Ionescu and Sofonea [8] using a complete implicit method for integration in time (see [18]).

If $(u, \boldsymbol{\sigma}^{\mathrm{R}})$ is the solution of the problem (9)–(13), then we determine:

$$\overline{u} = u - \tilde{u}, \quad \overline{\boldsymbol{\sigma}} = \boldsymbol{\sigma}^{\mathrm{R}} - \tilde{\boldsymbol{\sigma}}^{\mathrm{R}}, \tag{14}$$

such that

$$\begin{aligned} &\overline{u}(t, ma) = 0 \quad (\forall) t > 0, \\ &\operatorname{Div} \overline{\boldsymbol{\sigma}}(t, r) = 0 \quad (\forall) t > 0 \text{ and } r \in [a, ma], \\ &\overline{\boldsymbol{\sigma}}(t, a)\mathbf{n} = 0 \quad (\forall) t > 0. \end{aligned} \tag{15}$$

Thus, we have to solve the problem.

Find the displacement function $\overline{u}: \mathbf{R}_+ \times [a, ma] \to \mathbf{R}$, the stress function $\overline{\boldsymbol{\sigma}}: \mathbf{R}_+ \times [a, ma] \to \mathscr{S}_3$ and the irreversible stress work function $W^{\mathrm{I}}: \mathbf{R}_+ \times [a, ma] \to \mathbf{R}$ such that:

$$\begin{aligned} \dot{\overline{\boldsymbol{\sigma}}} = {} & 2G\mathfrak{e}(\dot{\overline{u}}) + (3K - 2G)\varepsilon(\dot{\overline{u}})\mathbf{1} + k_{\mathrm{T}} \left\langle 1 - \frac{W^{\mathrm{I}}(t)}{H(\overline{\boldsymbol{\sigma}} + \tilde{\boldsymbol{\sigma}} + \boldsymbol{\sigma}^{\mathrm{R}})} \right\rangle \left[\frac{(2G - 3K)}{3} \frac{\partial F}{\partial \sigma} (\overline{\boldsymbol{\sigma}} + \tilde{\boldsymbol{\sigma}} + \boldsymbol{\sigma}^{\mathrm{P}})\mathbf{1} \right. \\ & \left. - 2G \frac{\partial F}{\partial \boldsymbol{\sigma}} (\overline{\boldsymbol{\sigma}} + \tilde{\boldsymbol{\sigma}} + \boldsymbol{\sigma}^{\mathrm{P}}) \right] + k_{\mathrm{S}} \left[\frac{(2G - 3K)}{3} \frac{\partial S}{\partial \sigma} (\overline{\boldsymbol{\sigma}} + \tilde{\boldsymbol{\sigma}} + \boldsymbol{\sigma}^{\mathrm{P}})\mathbf{1} - 2G \frac{\partial S}{\partial \boldsymbol{\sigma}} (\overline{\boldsymbol{\sigma}} + \tilde{\boldsymbol{\sigma}} + \boldsymbol{\sigma}^{\mathrm{P}}) \right] \\ & \text{in } \mathbf{R}_+ \times [a, ma], \end{aligned} \tag{16}$$

$$\begin{aligned} \dot{W}^{\mathrm{I}} = {} & k_{\mathrm{T}} \left\langle 1 - \frac{W^{\mathrm{I}}(t)}{H(\overline{\boldsymbol{\sigma}} + \tilde{\boldsymbol{\sigma}} + \boldsymbol{\sigma}^{\mathrm{P}})} \right\rangle \frac{\partial F}{\partial \boldsymbol{\sigma}} (\overline{\boldsymbol{\sigma}} + \tilde{\boldsymbol{\sigma}} + \boldsymbol{\sigma}^{\mathrm{P}}) \cdot (\overline{\boldsymbol{\sigma}} + \tilde{\boldsymbol{\sigma}} + \boldsymbol{\sigma}^{\mathrm{P}}) \\ & + k_{\mathrm{S}} \frac{\partial S}{\partial \boldsymbol{\sigma}} (\overline{\boldsymbol{\sigma}} + \tilde{\boldsymbol{\sigma}} + \boldsymbol{\sigma}^{\mathrm{P}}) \cdot (\overline{\boldsymbol{\sigma}} + \tilde{\boldsymbol{\sigma}} + \boldsymbol{\sigma}^{\mathrm{P}}) \quad \text{in } \mathbf{R}_+ \times [a, ma], \end{aligned} \tag{17}$$

$$\begin{cases} \overline{\boldsymbol{\sigma}}(0, r) = 0, \\ \overline{u}(0, r) = 0, \\ W^{\mathrm{I}}(0, r) = H(\boldsymbol{\sigma}^{\mathrm{P}}), \end{cases} \quad (\forall) r \in [a, ma]. \tag{18}$$

In order to determine a numerical approach of the solution of the problem (16)–(18) we consider an interval $[0, T]$, $T > 0$.

Let us use the notation

$$\mathbf{V}_1 = \{v = (v_1, 0, 0) \mid v_1 \in L^2(\Omega),\ v_1 = v_1(r),\ v_1(ma) = 0\}, \tag{19}$$

$$\mathscr{V}_2 = \left\{\boldsymbol{\sigma} \in \left[L^2(\Omega)\right]_S^{3\times 3} \mid \boldsymbol{\sigma} = \boldsymbol{\sigma}(r),\ \mathrm{Div}\,\boldsymbol{\sigma} = 0 \text{ in } \Omega,\ \boldsymbol{\sigma}(a)\mathbf{n} = 0\right\}. \tag{20}$$

The solution $(\overline{u}, \overline{\boldsymbol{\sigma}}, W^{\mathrm{I}})$ of the problem (16)–(18) has the properties:

$$\overline{u} \in \mathbf{V}_1, \quad \overline{\boldsymbol{\sigma}} \in \mathscr{V}_2. \tag{21}$$

Let $M \in \mathbf{N}$, $M \geqslant 2$, $\Delta t = T/M$ be the step time and

$$t_0 = 0, \quad t_{n+1} = t_n + \Delta t, \quad n = \overline{0, M-1}. \tag{22}$$

Let us consider $\mathbf{V}_{\mathrm{h}} \subset \mathbf{V}_1$ a finite-dimensional subspace constructed using the finite element method. We will determine $\left(\overline{u}_{\mathrm{h}}^n, \overline{\boldsymbol{\sigma}}_{\mathrm{h}}^{n+1}, (W^{\mathrm{I}})_{\mathrm{h}}^{n+1}\right)$ approach of the solution $(\overline{u}, \overline{\boldsymbol{\sigma}}, W^{\mathrm{I}})$ on the moment t_n.

Let $\mathscr{B} = \{\varphi_1, \ldots, \varphi_{\mathrm{I}}\} \subset \mathbf{V}_{\mathrm{h}}$ be a base of $\mathbf{V}_{\mathrm{h}}$, dim $\mathbf{V}_{\mathrm{h}} = I$. Taking $\overline{u}_{\mathrm{h}}^0 = 0$ we determine $\overline{u}_{\mathrm{h}}^{n+1} \in \mathbf{V}_{\mathrm{h}}$, $n \geqslant 0$, such that:

$$\overline{u}_{\mathrm{h}}^{n+1} = \sum_{j=1}^{I} \alpha_j^{n+1} \varphi_j, \tag{23}$$

where the constants α_j^{n+1}, $j = \overline{1, I}$ are the solution of the linear system:

$$\sum_{j=1}^{I} R_{ij} \tilde{\alpha}_j^{n+1} = \sum_{j=1}^{I} R_{ij} \tilde{\alpha}_j^n - \Delta t\, T_i, \quad i = \overline{1, I}, \tag{24}$$

where

$$\tilde{\alpha}_j^n = \frac{\alpha_j^n}{a}, \quad j = \overline{1, I},$$

$$R_{ij} = \frac{3K + 4G}{3}\left(\int_1^m s \frac{\partial \varphi_j}{\partial s}\frac{\partial \varphi_i}{\partial s}\,\mathrm{d}s + \int_1^m \frac{1}{s}\varphi_j\varphi_i\,\mathrm{d}s\right) + \frac{3K - 2G}{3}\int_1^m \left(\varphi_j \frac{\partial \varphi_i}{\partial s} + \frac{\partial \varphi_j}{\partial s}\varphi_i\right)\mathrm{d}s, \quad i,j = \overline{1, I},$$

$$T_i = k_{\mathrm{T}}\left\{\int_1^m s\left\langle 1 - \frac{(W^{\mathrm{I}})_{\mathrm{h}}^n}{H(\overline{\boldsymbol{\sigma}}_{\mathrm{h}}^n + \tilde{\boldsymbol{\sigma}} + \boldsymbol{\sigma}^{\mathrm{P}})}\right\rangle \left[\frac{2G - 3K}{3}\frac{\partial F}{\partial \sigma}(\overline{\boldsymbol{\sigma}}_{\mathrm{h}}^n + \tilde{\boldsymbol{\sigma}} + \boldsymbol{\sigma}^{\mathrm{P}}) - 2G\frac{\partial F}{\partial \sigma_{rr}}(\overline{\boldsymbol{\sigma}}_{\mathrm{h}}^n + \tilde{\boldsymbol{\sigma}} + \boldsymbol{\sigma}^{\mathrm{P}})\right]\frac{\partial \varphi_i}{\partial s}\,\mathrm{d}s \right.$$
$$\left. + \int_1^m \left\langle 1 - \frac{(W^{\mathrm{I}})_{\mathrm{h}}^n}{H(\overline{\boldsymbol{\sigma}}_{\mathrm{h}}^n + \tilde{\boldsymbol{\sigma}} + \boldsymbol{\sigma}^{\mathrm{P}})}\right\rangle \left[\frac{2G - 3K}{3}\frac{\partial F}{\partial \sigma}(\overline{\boldsymbol{\sigma}}_{\mathrm{h}}^n + \tilde{\boldsymbol{\sigma}} + \boldsymbol{\sigma}^{\mathrm{P}}) - 2G\frac{\partial F}{\partial \sigma_{\theta\theta}}(\overline{\boldsymbol{\sigma}}_{\mathrm{h}}^n + \tilde{\boldsymbol{\sigma}} + \boldsymbol{\sigma}^{\mathrm{P}})\right]\varphi_i\,\mathrm{d}s \right\}$$

$$+k_S\left\{\int_1^m s\left[\frac{2G-3K}{3}\frac{\partial S}{\partial\sigma}(\overline{\boldsymbol{\sigma}}_h^n+\tilde{\boldsymbol{\sigma}}+\boldsymbol{\sigma}^P)-2G\frac{\partial S}{\partial\sigma_{rr}}(\overline{\boldsymbol{\sigma}}_h^n+\tilde{\boldsymbol{\sigma}}+\boldsymbol{\sigma}^P)\right]\frac{\partial\varphi_i}{\partial s}\,ds\right.$$
$$\left.+\int_1^m\left[\frac{2G-3K}{3}\frac{\partial S}{\partial\sigma}(\overline{\boldsymbol{\sigma}}_h^n+\tilde{\boldsymbol{\sigma}}+\boldsymbol{\sigma}^P)-2G\frac{\partial S}{\partial\sigma_{\theta\theta}}(\overline{\boldsymbol{\sigma}}_h^n+\tilde{\boldsymbol{\sigma}}+\boldsymbol{\sigma}^P)\right]\varphi_i\,ds\right\},\quad i=\overline{1,I}.$$

For the stress approach and irreversible stress work approach we consider $\overline{\boldsymbol{\sigma}}_h^0=0$ and $(W^I)_h^0=H(\boldsymbol{\sigma}^P)$ and we determine $\left(\overline{\boldsymbol{\sigma}}_h^{n+1}\right)_{n\geqslant 0}$ and $\left((W^I)_h^{n+1}\right)_{n\geqslant 0}$ using the following implicit scheme:

$$\begin{aligned}\overline{\boldsymbol{\sigma}}_h^{n+1}&=\overline{\boldsymbol{\sigma}}_h^n+2G\left[\boldsymbol{\varepsilon}(\overline{u}_h^{n+1})-\boldsymbol{\varepsilon}(\overline{u}_h^n)\right]-(3K-2G)\left[\varepsilon(\overline{u}_h^{n+1})-\varepsilon(\overline{u}_h^n)\right]\mathbf{1}\\&+\Delta t\,k_T\left\langle 1-\frac{(W^I)_h^{n+1}}{H(\overline{\boldsymbol{\sigma}}_h^{n+1}+\tilde{\boldsymbol{\sigma}}+\boldsymbol{\sigma}^P)}\right\rangle\left[\frac{(2G-3K)}{3}\frac{\partial F}{\partial\sigma}(\overline{\boldsymbol{\sigma}}_h^{n+1}+\tilde{\boldsymbol{\sigma}}+\boldsymbol{\sigma}^P)\mathbf{1}\right.\\&\left.-2G\frac{\partial F}{\partial\boldsymbol{\sigma}}(\overline{\boldsymbol{\sigma}}_h^{n+1}+\tilde{\boldsymbol{\sigma}}+\boldsymbol{\sigma}^P)\right]+\Delta t\,k_S\left[\frac{(2G-3K)}{3}\frac{\partial S}{\partial\sigma}(\overline{\boldsymbol{\sigma}}_h^{n+1}+\tilde{\boldsymbol{\sigma}}+\boldsymbol{\sigma}^P)\mathbf{1}\right.\\&\left.-2G\frac{\partial S}{\partial\boldsymbol{\sigma}}(\overline{\boldsymbol{\sigma}}_h^{n+1}+\tilde{\boldsymbol{\sigma}}+\boldsymbol{\sigma}^P)\right],\end{aligned}\tag{25}$$

and, respectively,

$$\begin{aligned}(W^I)_h^{n+1}&=(W^I)_h^n+\Delta t\,k_T\left\langle 1-\frac{(W^I)_h^{n+1}}{H(\overline{\boldsymbol{\sigma}}_h^{n+1}+\tilde{\boldsymbol{\sigma}}+\boldsymbol{\sigma}^P)}\right\rangle\frac{\partial F}{\partial\sigma}(\overline{\boldsymbol{\sigma}}_h^{n+1}+\tilde{\boldsymbol{\sigma}}+\boldsymbol{\sigma}^P)(\overline{\boldsymbol{\sigma}}_h^{n+1}+\tilde{\boldsymbol{\sigma}}+\boldsymbol{\sigma}^P)\\&+\Delta t\,k_S\frac{\partial S}{\partial\sigma}(\overline{\boldsymbol{\sigma}}_h^{n+1}+\tilde{\boldsymbol{\sigma}}+\boldsymbol{\sigma}^P)(\overline{\boldsymbol{\sigma}}_h^{n+1}+\tilde{\boldsymbol{\sigma}}+\boldsymbol{\sigma}^P).\end{aligned}\tag{26}$$

5. Numerical results

In order to construct the space $\mathbf{V}_h$, referring to functions $\overline{u}$, $\overline{\boldsymbol{\sigma}}$, W^I which depend of the variable r only (these functions are independent on the variable θ), we will consider that the interval $[1,m]$ was divided into 100 linear elements with $m=10$ or $m=15$. The time step was considered 1/100 dimensionless time unit or 1/200 dimensionless time unit. The dimensionless time T is time divided by the constant k_S. In numerical calculus we consider $k_T=5\times10^{-6}$ s^{-1} and $k_S=3\times10^{-5}$ s^{-1}.

If we assume that after excavation the stresses remain constant (as in creep tests) then the convergence of the borehole by creep is obtained from [4,5]:

$$\frac{u}{a}=-\frac{p-\sigma_h}{2G}\frac{a}{r}+\frac{r}{a}\left\{\frac{\langle 1-(W_T(t_0)/H)\rangle\partial F/\partial\sigma_\theta}{(1/H)(\partial F/\partial\boldsymbol{\sigma})\cdot\boldsymbol{\sigma}}\left\{1-\exp\left[\frac{k_T}{H}\frac{\partial F}{\partial\boldsymbol{\sigma}}\cdot\boldsymbol{\sigma}(t_0-t)\right]\right\}+k_S\frac{\partial S}{\partial\sigma_\theta}(t-t_0)\right\},\tag{27}$$

where $W_T(t_0)$ stays for the initial "primary" value of W_T. If the initial, primary, stress state is an equilibrium state then $W_T(t_0=H(\boldsymbol{\sigma}^P)$.

Fig. 1 shows the radial convergence u of a borehole excavated at depth $h=400$ m when the far field stresses ratio $\sigma_h/\sigma_v=n=1$, $\sigma_h=10$ MPa and the inner surface is subjected to a pressure

shown (due to a brine column, or some other reason). Three solutions are shown. The curve marked E is the elastic solution, i.e., the initial convergence just after excavation. The solution S corresponds to the "simplified" solution (27) obtained after a dimensionless time interval $T = 5.2 \times 10^2$ (with the numerical value of the viscosity coefficient we have considered here that would correspond to about 200 days). The numerical solution N obtained by the finite element calculation and which takes into account the stress variation during creep, is quite close to the simplified solution S. The corresponding stress variation is shown in Fig. 2. The upper curves correspond to the distribution of σ_θ, while the lower curves to σ_r. The component σ_z ($= \sigma_h$ in the

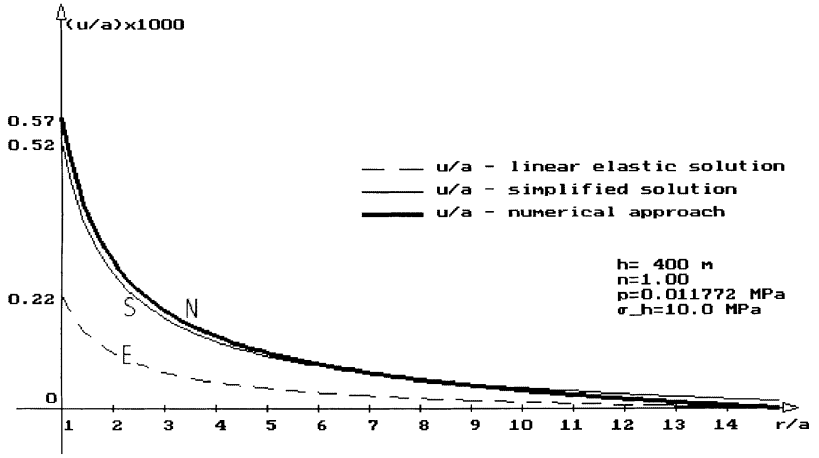

Fig. 1. The radial convergence of a borehole excavated at $h = 400$ m for $n = 1$.

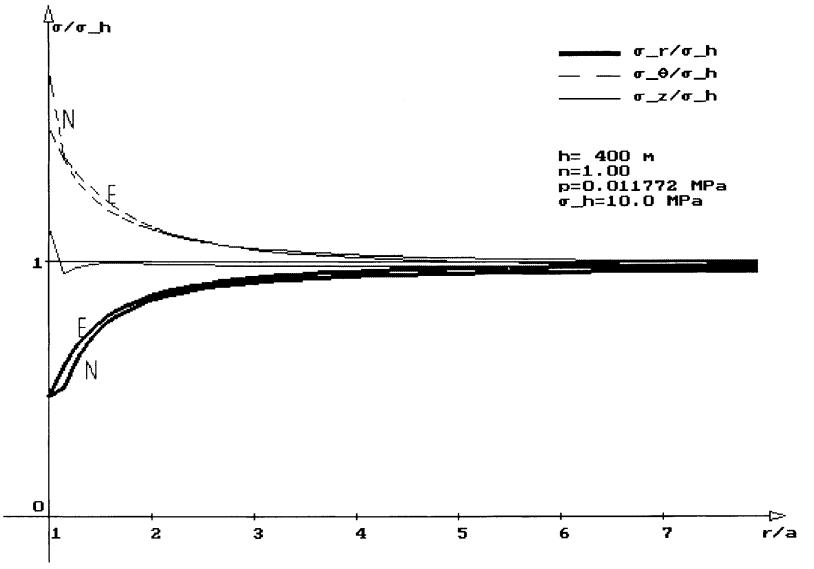

Fig. 2. Stress variation around a borehole excavated at $h = 400$ m for $n = 1$.

elastic solution) does not vary much in the numerical solution. Close to the borehole surface in the numerical solution, σ_θ is greater than in the elastic solution, while σ_r is smaller.

At greater depth, mainly if the ratio n is no more equal to one, the three solutions are quite distinct. Fig. 3 shows the radial convergence at depth $h = 1200$ m, for $n = 0.7$, $p = 0.011772$ MPa and $\sigma_h = 21.0$ MPa. The elastic, instantaneous convergence E is compared with the numerical solution N and the simplified one S. The solutions N and S have been obtained for dimensionless time $T = 7.8 \times 10^3$. The corresponding stress distribution is shown in Fig. 4. The numerical solution N is compared with the elastic one (not marked lines). One can see that at greater depth the numerical solution departs significantly from the initial elastic one.

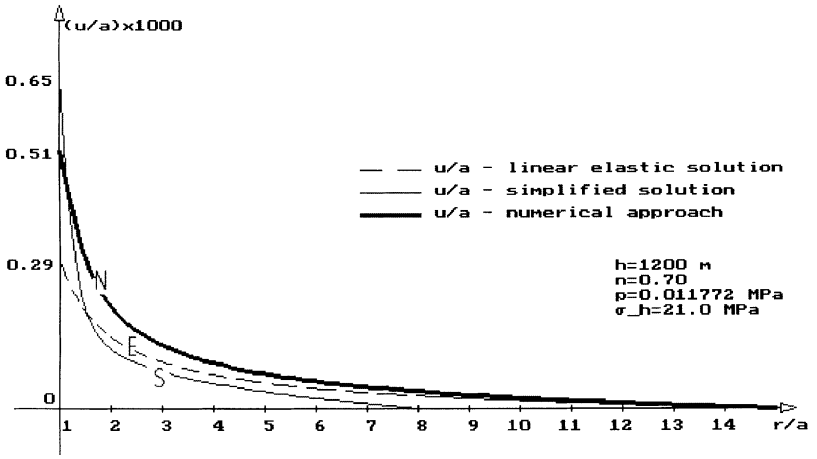

Fig. 3. The radial convergence of a borehole excavated at $h = 1200$ m for $n = 0.7$.

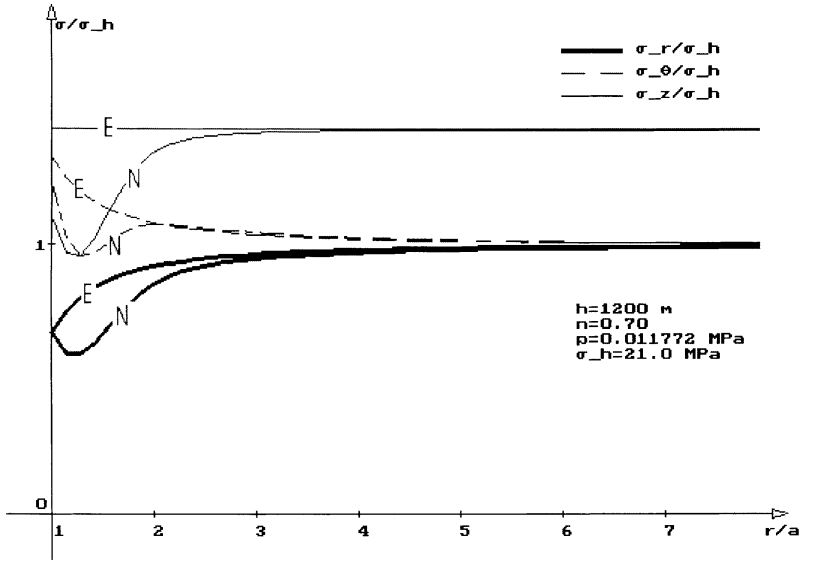

Fig. 4. Stress variation around a borehole excavated at $h = 1200$ m for $n = 0.7$.

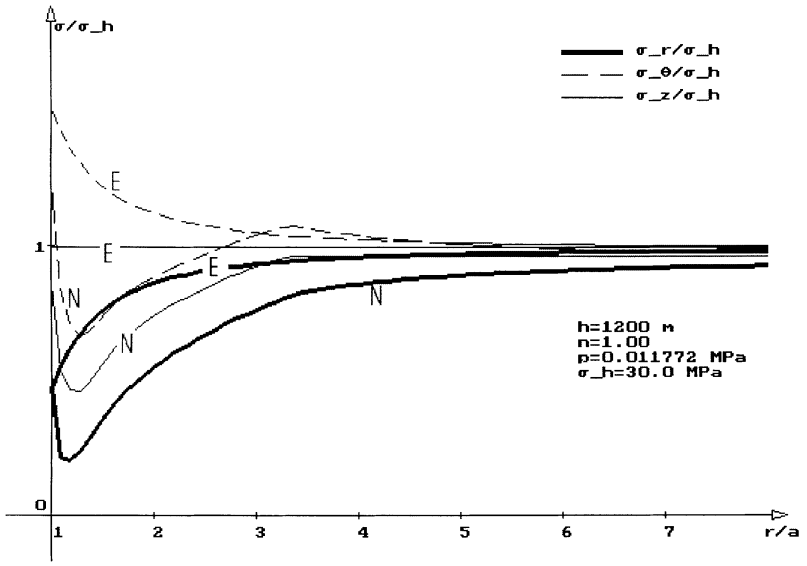

Fig. 5. Stress variation around a borehole excavated at $h = 1200$ m for $n = 1$.

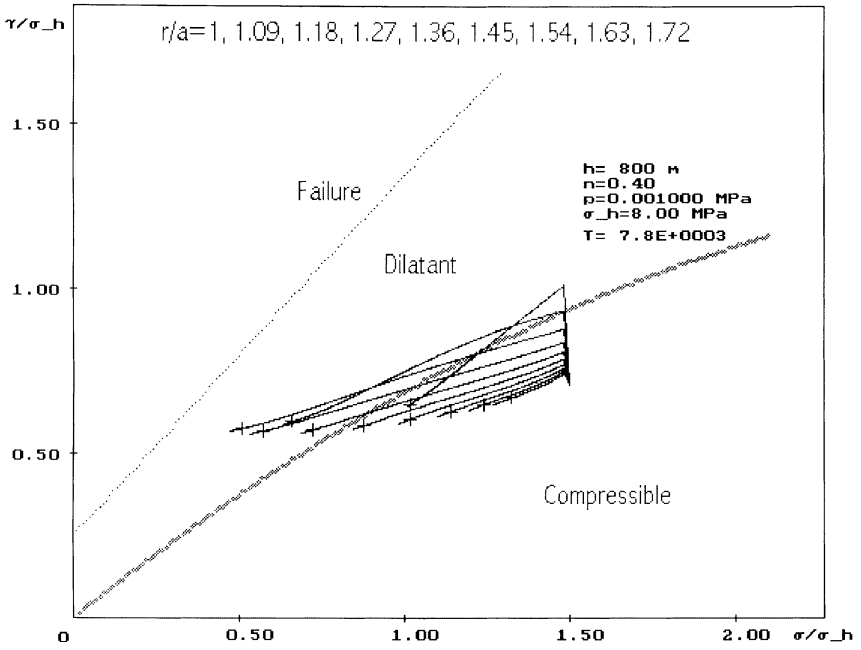

Fig. 6. Stress variation in a $\sigma\tau$-plane at $h = 800$ m.

Also, generally in the neighborhood of the borehole surface the stresses "relaxe". This "relaxation" can be seen also on Fig. 5 corresponding to the same depth $h = 1200$ m but for $n = 1$ and $\sigma_h = 30$ MPa. Again, after excavation all components of the stress decrease in the neighborhood of the borehole surface. This "relaxation" of the stress components in long time intervals following excavation, will further be investigated in order to find out the consequences for the borehole stability.

The stress variation during creep, following the drilling of the borehole can be shown in a $\sigma\tau$-plane, where the compressibility/dilatancy boundary and the short-term failure condition are also shown. Fig. 6 shows the stress relaxation around a borehole drilled at depth $h = 800$ m for the ratio of far field stresses $\sigma_h/\sigma_v = n = 0.4$ and for a small inner pressure p. Just after excavation the stress state at various distances from the wall are represented by points located on the vertical line shown. After excavation both τ and σ decrease by slow relaxation. The upper inclined line shows the relaxation at $r = a$ the next one for $r = 1.09a$, etc. For $r > 2a$ the stress variation is very small. The crosses on these curves are showing up to where both transient and steady-state terms are contributing to the stress relaxation. Beyond these crosses only the steady-state terms have a significant contribution. The computations have been carried out for the dimensionless time $T = 7.8 \times 10^3$ (if we estimate $k_s = 3 \times 10^{-5}$ that would correspond to slightly more than eight years). Generally the stress variation shown in Fig. 6 is not endangering the stability of the borehole, at least for the time interval considered. As a rule, the depth and value of σ_h influence significantly the stability of the borehole; an added inner pressure is generally contributing to the stability.

Fig. 7 shows another interesting case, when close to the borehole wall both τ and σ decrease, but at slightly greater distances σ decreases but τ increases. Also this figure shows that after the time

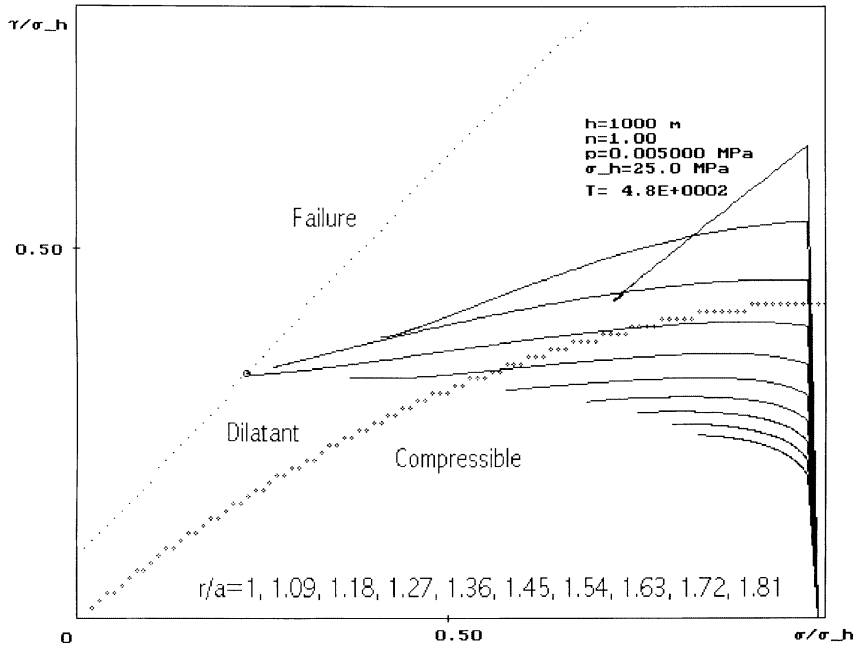

Fig. 7. Stress variation in a $\sigma\tau$-plane at $h = 1000$ m for $p = 0.005$ MPa.

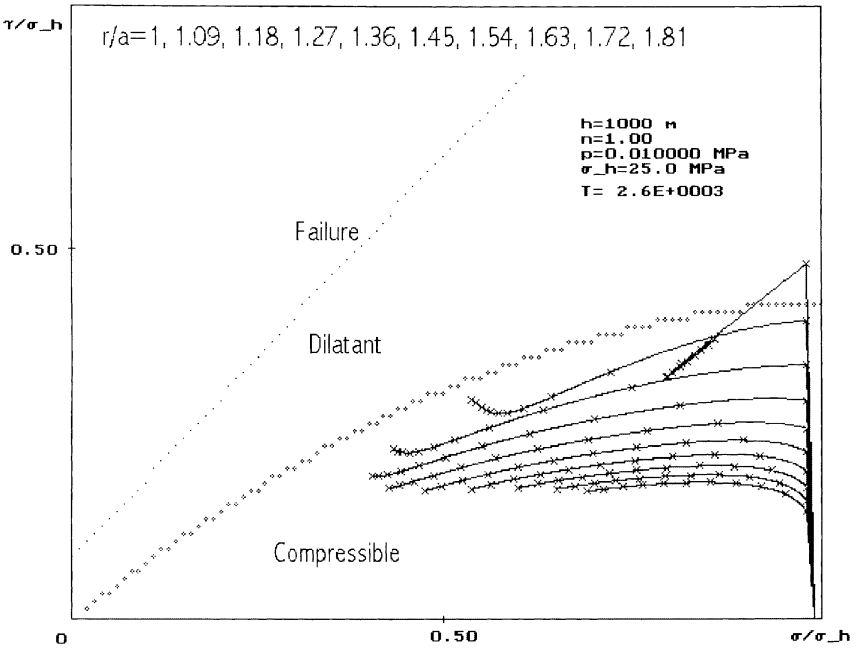

Fig. 8. Stress variation in a $\sigma\tau$-plane at $h = 1000$ m for $p = 0.01$ MPa.

$T = 5 \times 10^2$ at distance $r = 1.27a$ from the borehole surface, the short-term failure surface will be reached, i.e., a sudden failure is possible after a long time interval, and this failure is predicted to take place at a certain distance from the borehole wall. An increased inner pressure contributes to the stability; we have found that by doubling the inner pressure the time necessary for the stress variation to reach the short-term failure surface is increased with one order of magnitude and the failure takes place at greater distances from the borehole wall. In the same manner, if the inner pressure is significantly increased the borehole becomes completely stable for a very long time interval (see Fig. 8).

The stars on the curves shown in Fig. 8 mark equal intervals of time; thus, the stress variation is quite fast at the beginning (just after excavation), and the speed of the variation steadily decreases, mainly in the neighborhood of the borehole.

Fig. 9 shows for greater depths the stress relaxation after borehole drilling. The inner pressure corresponds to that of a column of brine and $n = 1$. This case is quite stable, during variation in time, the stresses remain in the compressibility domain and no failure is predicted for a long period of time. However, at the same depth, if the ratio of the far field stresses are distinct from one and the inner pressure is much smaller, the conclusion may be quite different. For instance, Fig. 10 shows a similar case as in Fig. 9 but for $n = 0.75$. This time the stress states around the borehole are in the dilatant region. Even the stress states (at $r = 2.81a$, say) initially in the compressibility domain are steadily moving towards the dilatancy domain. Furthermore, by slow stress relaxation around the borehole, sudden failure may occur at $r = 1.9a$ after a time interval of $T = 1.6 \times 10^2$. Again we find that it is at a certain distance from the borehole wall that failure is taking place.

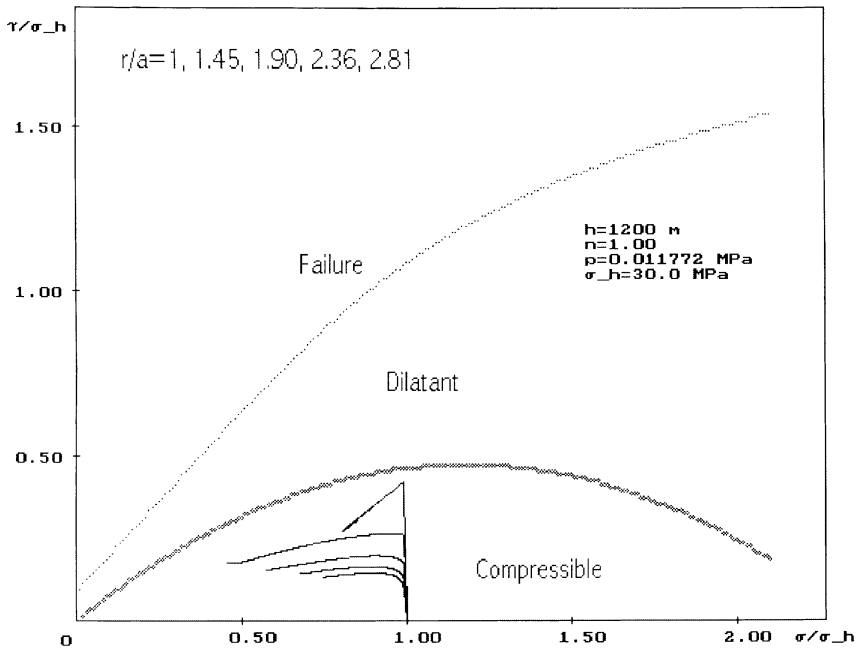

Fig. 9. Stress variation in a $\sigma\tau$-plane at $h = 1200$ m for $n = 1$.

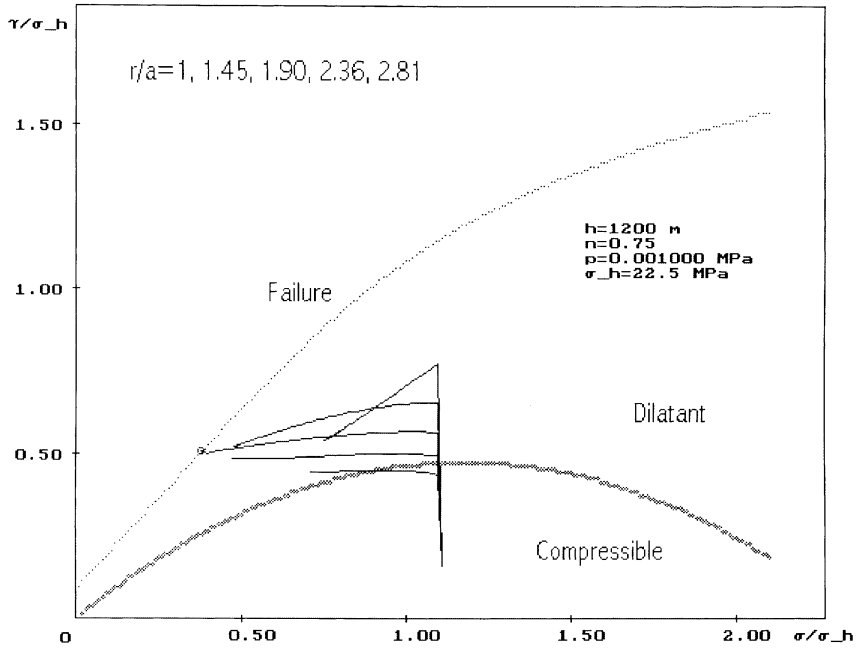

Fig. 10. Stress variation in a $\sigma\tau$-plane at $h = 1200$ m for $n = 0.75$.

6. Conclusions

The conclusions for displacement and stress distribution around a borehole excavated in rock salt are compared: the elastic solution (E), the simplified solution assuming stress constancy during creep (S), and a numerical solution (N) taking into account the stress variation during creep closure of the borehole. It is shown that at relative small depth, and ratio of far field stress $n = 1$, the solutions S and N are quite close and thus the first estimation of the borehole convergence can be obtained with a very simple formula. At greater depths and for $n \neq 1$ a numerical solution (N) which makes no simplifying assumption is needed. Also, it is shown that in long time intervals a sudden failure is possible due to the slow variation of the stresses. This problem will farther be investigated.

Appendix A

This example for the constitutive functions for rock salt is presented in [4]. Function $H(\boldsymbol{\sigma})$ is

$$H(\sigma,\tau) = \left[a_1 + \frac{a_2}{(\sigma/\sigma_*)^6}\right]\left(\frac{\tau}{\sigma_*}\right)^{14} + \left(b_1\frac{\sigma}{\sigma_*} + b_2\right)\left(\frac{\tau}{\sigma_*}\right)^3 + \left[\frac{c_1}{(\sigma/\sigma_*)^3 + c_3} + c_2\right]\frac{\tau}{\sigma_*} + \begin{cases} h_1\left[1 - \cos\left(\omega\frac{\sigma}{\sigma_*}\right)\right] & \text{if } 0 < \sigma < \sigma_0, \\ 2h_1 & \text{if } \sigma \geqslant \sigma_0, \end{cases}$$

where $a_1 = 7 \times 10^{-21}$ MPa, $a_2 = 6.73 \times 10^{-12}$ MPa, $b_1 = 1.572 \times 10^{-6}$ MPa, $b_2 = 1.766 \times 10^{-5}$ MPa, $c_1 = 26.123$ MPa, $c_2 = -0.00159$ MPa, $c_3 = 3134$, $h_1 = 0.118$ MPa, $\omega = 3.4°$, $\sigma_0 = 53$ MPa, $\sigma_* = 1$ MPa.

The failure boundary has the equation:

$$Y(\sigma,\tau) = -r\frac{\tau}{\sigma_*} - s\left(\frac{\tau}{\sigma_*}\right)^6 + t_0 + \frac{\sigma}{\sigma_*} = 0,$$

where $r = 0.9$, $s = 1.025 \times 10^{-8}$, $t_0 = 1.82$.

The compressibility/dilatancy boundary has the equation:

$$X(\sigma,\tau) = -\frac{\tau}{\sigma_*} + f_1\left(\frac{\sigma}{\sigma_*}\right)^2 + f_2\frac{\sigma}{\sigma_*} = 0,$$

where $f_1 = -0.01526$ and $f_2 = 0.8088$.

The function F is obtained from:

$$k_T\frac{\partial F}{\partial \sigma} = \begin{cases} \frac{X(\sigma,\tau)\left[p_1(\sigma/\sigma_*)^2 + p_2(\sigma/\sigma_*) + p_3\right]}{Y(\sigma,\tau)}\left[G_1(\tau) + 1\right] & \text{if } 0 < \sigma < \sigma_0, \\ 0 \quad \text{if } \sigma \geqslant \sigma_0, \end{cases}$$

where $p_1 = -9.83 \times 10^{-7}$ s^{-1}, $p_2 = -5.226 \times 10^{-5}$ s^{-1}, $p_3 = 9.84 \times 10^{-5}$ s^{-1} and

$$G_1(\tau) = u_1 \frac{\tau}{\sigma_*} + u_2 \left(\frac{\tau}{\sigma_*} \right)^2 + u_3 \left(\frac{\tau}{\sigma_*} \right)^3 + u_4 \left(\frac{\tau}{\sigma_*} \right)^8,$$

where $u_1 = 0.0365$, $u_2 = -0.00265$, $u_3 = 5.256 \times 10^{-5}$, $u_4 = 1.576 \times 10^{-12}$.

The expression of the viscoplastic potential F is

$$\begin{aligned} k_T F(\sigma,\tau) = {} & \left\{ \frac{f_1 p_1}{4} [Y(\sigma,\tau)]^4 + \left[-\frac{4}{3} f_1 p_1 B(\tau) + \frac{1}{3}(f_2 p_1 + f_1 p_2) \right] [Y(\sigma,\tau)]^3 \right. \\ & + \left\{ 3 f_1 p_1 [B(\tau)]^2 - \frac{3}{2}(f_2 p_1 + f_1 p_2) B(\tau) + \frac{1}{2} \left(f_2 p_2 + f_1 p_3 - \frac{\tau}{\sigma_*} p_1 \right) \right\} [Y(\sigma,\tau)]^2 \\ & + \left\{ -4 f_1 p_1 [B(\tau)]^3 + 3(f_2 p_1 + f_1 p_2)[B(\tau)]^2 - \left(f_2 p_2 + f_1 p_3 - \frac{\tau}{\sigma_*} p_1 \right) B(\tau) \right\} Y(\sigma,\tau) \\ & + \left\{ f_1 p_1 [B(\tau)]^4 - (f_2 p_1 + f_1 p_2)[B(\tau)]^3 + \left(f_2 p_2 + f_1 p_3 - \frac{\tau}{\sigma_*} p_1 \right) [B(\tau)]^2 \right. \\ & \left. \left. - \left(f_2 p_3 - \frac{\tau}{\sigma_*} p_2 \right) B(\tau) - \frac{\tau}{\sigma_*} p_3 \right\} \ln Y(\sigma,\tau) + \left(f_2 p_3 - \frac{\tau}{\sigma_*} p_2 \right) \frac{\sigma}{\sigma_*} \right\} \sigma_* [G_1(\tau) + 1] + g(\tau) \end{aligned}$$

where

$$B(\tau) = -r \frac{\tau}{\sigma_*} - s \left(\frac{\tau}{\sigma_*} \right)^6 + t_0, \quad g(\tau) = g_0 \frac{\tau}{\sigma_*} + \frac{g_1}{2} \left(\frac{\tau}{\sigma_*} \right)^2 + \frac{g_2}{4} \left(\frac{\tau}{\sigma_*} \right)^4$$

and $g_0 = 0.0108$ MPa/s, $g_1 = 6.582 \times 10^{-5}$ MPa/s, $g_2 = 5.954 \times 10^{-6}$ MPa/s.

The stationary viscoplastic potential S is

$$k_S S(\sigma,\tau) = \left\{ \begin{array}{l} b \left(\frac{\tau}{\sigma_*} \right)^m \left(\frac{\sigma}{\sigma_*} \right)^{n+1} \frac{\sigma_*}{n+1} + Q\left(\frac{\tau}{\sigma_*} \right) \quad \text{if} \left\{ \begin{array}{l} \tau > \tau_m \\ \text{or} \\ \sigma \leqslant \sigma_a \text{ and } \tau \leqslant \tau_m \end{array} \right. \\ b \left(\frac{\tau}{\sigma_*} \right)^m \left(\frac{\sigma_a}{\sigma_*} \right)^{n+1} \frac{\sigma_*}{n+1} + Q\left(\frac{\tau}{\sigma_*} \right) \quad \text{if } \sigma_a \leqslant \sigma \leqslant \sigma_b \\ b \left(\frac{\tau}{\sigma_*} \right)^m \frac{\sigma_*}{n+1} \left[\left(\frac{\sigma_a}{\sigma_*} \right)^{n+1} - \left(\frac{\sigma_b}{\sigma_*} \right)^{n+1} \right. \\ \left. + \left(\frac{\sigma}{\sigma_*} \right)^{n+1} \right] + Q\left(\frac{\tau}{\sigma_*} \right), \quad \text{if } \sigma_b \leqslant \sigma \end{array} \right\} \text{and } \tau \leqslant \tau_m,$$

where $b = -1 \times 10^{-14}$ s^{-1}, $m = 5$, $n = -0.1$,

$$\left.\begin{matrix}\sigma_a/\sigma_* \\ \sigma_b/\sigma_*\end{matrix}\right\} = \frac{-f_2 \pm \sqrt{f_2^2 + 4f_1(\tau/\sigma_*)}}{2f_1}, \quad \tau_m = -\frac{f_2^2}{4f_1},$$

and

$$Q'\left(\frac{\tau}{\sigma_*}\right) = \frac{p}{\sigma_*}\left(\frac{\tau}{\sigma_*}\right)^5,$$

where $p = 4.256 \times 10^{-13}$ MPa/s.

References

[1] N. Cristescu, Fluage, Dilatance et/ou Compressibilité des Roches autour des Puits Verticaux et des Forages Petroliers, Revue Francaise de Geotechnique 31 (1985) 11–22.
[2] N. Cristescu, Viscoplastic creep of rocks around horizontal tunnels, Int. J. Rock Mec. Min. Sci. Geomech. Abstr. 22 (6) (1985) 453–459.
[3] N. Cristescu, Rock Rheology, Kluwer Academic Publishers, Dordrecht, 1989.
[4] N. Cristescu, in: N.D. Cristescu, G. Gioda (Eds.), Viscoplasticity of Geomaterials, Visco-plastic Behavior of Geomaterials, Springer, Wien-New York, 1994, pp. 103–207.
[5] N.D. Cristescu, U. Hunsche, Time Effects in Rock Mechanics, Wiley, New York, 1998.
[6] W. Dreyer, The Science of Rock Mechanics. Part 1: The Strength Properties of Rocks, Trans Tech Publ, Clausthal-Zellerfeld, 1972.
[7] U. Glabisch, Stoffmodell fur Grenzzustande im Salzgestein zur Berechnung von Gebirgshohlraumen, Ph.D. Dissertation, Technical University Carolo, Wilhelmina, Braunschweig, Germany, 1997.
[8] I.R. Ionescu, M. Sofonea, Functional and Numerical Methods in Viscoplasticity, Oxford University Press, Oxford, 1993.
[9] J. Jin, N.D. Cristescu, An elastic/viscoplastic model for transient creep of rock salt, Int. J. Plasticity 14 (1998) 85–107.
[10] A.R. Jumikis, Rock Mechanics, Trans Tech Publ, Clausthal-Zellerfeld, 1979.
[11] B. Ladanyi, Time-dependent response of rock around tunnels, in: J.A. Hudson (Ed.-in-Chief), Comprehensive Rock Engineering, Analysis and Design Methods, vol. 2, Pergamon Press, Oxford, 1993, pp. 77–112.
[12] D. Massier, Creep of linear viscoelastic rock around a circular cylindrical excavation in the case of general far field stresses, Studii si Cercetari de Mecanica Aplicata 53 (5) (1994) 427–442.
[13] D. Massier, Rock Mechanics, University of Bucharest, 1997.
[14] D. Massier, N. Cristescu, In situ creep of rocks, Rev. Roumaine Sci. Techn. Ser. Mec. Appl. 26 (5) (1981) 687–702.
[15] A.A. Matei, N.D. Cristescu, The effect of volumetric strain on elastic parameters for rock salt, Mechanics of Cohesive-Frictional Materials 4 (1999).
[16] L. Obert, W.I. Duvall, Rock Mechanics and the Design of Structures in Rock, Wiley, New York, 1967.
[17] I. Paraschiv, N. Cristescu, Deformability response of rock salt around circular mining excavations, Rev. Roumaine Sci. Techn. Mec. Appl. 38 (3) (1993) 257–276.
[18] I. Paraschiv-Munteanu, Metode numerice in geomecanica, Ph.D. Dissertation, University of Buchasrest, Romania, 1997.
[19] J. Prij, J.J. Heijdra, B.A. van den Horn, Convergence and compaction of backfilled openings in rocksalt, in: M. Ghoreychi, P. Berest, H.R. Hardy, Jr., M. Langer (Eds.), The Mechanical Behavior of Salt. Proceedings of the Third Conference, Trans Tech Publ., Clausthal-Zellerfeld, 1996, pp. 337–350.

[20] G. Staupendahl, M.W. Schmidt, M.W. Meister, M. Wallner, Geotechnical investigations in the prototype cavity in the ASSE salt mine, in: Proceedings of the Fourth International Congress on Rock Mechanics, vol. III, Balkema, Rotterdam, 1979, pp. 645–653.
[21] R.P. Steiger, P.K. Leung, Advances in shale mechanics – the key to wellbore stability predictions, in: J.A. Hudson (Ed.-in-Chief), Comprehensive Rock Engineering, Surface and Underground Case Histories, vol. 5, Pergamon Press, Oxford, 1993, pp. 629–639.